© Universiti Tun Hussein Onn Malaysia Publisher's Office

IJIE

Journal homepage: http://penerbit.uthm.edu.my/ojs/index.php/ijie
ISSN : 2229-838X e-ISSN : 2600-7916

The International Journal of Integrated Engineering

Experimental Evaluation and Analysis of LED Illumination Source for Endoscopy Imaging

Hiren Mewada[1*], Amit Patel[2], Jitendra Chaudhari[2], Keyur Mahant[2], Alpesh Vala[2]

[1]Hiren Mewada, Electrical Engineering Department,
Prince Mohammad Bin Fahd University, Al Khobar, Kingdom of SAUDI ARABIA

[2]Amit Patel, Jitendra Chaudhari, Keyur Mahant, Alpesh Vala
CHARUSAT Space Research and Technology Center, Charotar University of Science & Technology, Changa, Gujarat, INDIA

*Corresponding Author

DOI: https://doi.org/10.30880/ijie.2022.14.04.020
Received 24 May 2021; Accepted 17 April 2022; Available online 20 June 2022

Abstract: The minimally invasive surgery uses a small instrument with camera and light to fit the tiny cut in the skin. The selection of the light depends on the power and driving current of the circuit. It can also help in the standardization of the camera and capture the tissues' true-colour image. This paper presents the LED source analysis used in the clinical endoscopes for surgery and the human body's medical examination. Initially, a LED source selection mechanism generating intense illuminance in a visible band is proposed. A low-cost prototype model is developed to analyze the wavelength and illuminance of three different LEDs types. An effect on variation in LED illumination is investigated by changing the distance between the Borescope and LED source. True-colour image generation and tissue contrast are more important in medical diagnostics. Therefore, a sigmoid function improving the whole contrast ratio of the captured image in real-time is presented. The results of spectrum and wavelength for a current variation are presented. Type 3 LED produces higher illumination (i.e., 395 Klux) and peak wavelength (i.e., 622.05 nm) than other LEDs, while type-2 LED has better FWHM for the blue colour spectrum. The modification in the sigmoid function enhances the image with 34.25 peak PSNR producing a true-colour image.

Keywords: Light emitting diode, spectrum analysis, endoscopy, contrast enhancement

1. Introduction

In surgery, minimally invasive techniques (MIT) are generally safer than open surgery and typically faster recovery. This biological photographic surgery has increased interest in LED-based treatments. LEDs have now become essential in medical and dental technology. But the demands placed on these devices are extreme. Minimal size, large and application-specific colour rendering index, efficient temperature control, usability, and excellent disinfection opportunities are all important.

An endoscopy is a process where the doctor uses specialized instruments to look and operate on the body's internal parts like organs and vessels. It allows experts to view disease within the body without making a large body cut. Endoscopy surgery requires an average of 45 minutes. It involves the use of an external illumination source. Considering intense illuminance and colour rendering index (Ra) greater than 95, Xenon, Halogen, and Metal halide lamps are recently used as an illumination source in minimally invasive techniques. These sources emit a broad visible frequency spectrum,

*Corresponding author: hmewada@pmu.edu.sa

producing natural colours like daylight. Sometimes, filters are also incorporated to keep the desired wavelength from the source. However, a traditional lighting system generates heat, resulting in energy wastage and a short lifespan.

Nowadays, LEDs are replacing the Xenon lamps in medical devices due to their inherent advantages like small in size, less in cost, energy efficiency, robustness, and can be calibrated in the visible range for their spectral emission [1]. Wehby et al. [2] presented a design of 100 watts LED source for medical endoscopy. They simulated their model in MATLAB, but physical implementation is not done yet. Traditional endoscopy is costlier, and the high cost of endoscopy may limit its use in under-development countries. Therefore, a portable, self-contained LED source is designed [3]. They distributed this device among urologists, and from the feedback of the urologist, an analysis is presented to use low-cost portable equipment in surgery. Furthermore, efficacy comparison of blue light imaging using an LED light source and LASER light source for early gastric cancer diagnostic was presented in [4]. They concluded that imaging obtained using blue light of LED provided better visualization and was not inferior to LASER.

A laparoscopic system was developed by Mueller et al. [5]. They evaluated this system using traditional imaging systems. They replaced the expensive fiber optic with the small size of LED, and the CMOS detector is used for imaging. They performed thermal testing and image quality evaluation. The thermal testing was done at the interval of 10 min over a 90 min period, and they observed that it does not exceed 48oC of temperature. Siqueira et al. [6] presented an integrated approach for light control in video laparoscopy. They developed a device controlling the LED light where up to 450 lm intensity was obtained with daylight LED and up to 672 lm intensity was obtained using white light LED.

An algorithm using encoded LED light to display ureter position was presented in [7]. The image was captured using an encoded LED and processed further using the monochrome channel filtering method to make it more precise and succeeded with 92.04% region. The LED endoscope was compared with the LASER endoscope in [8]. They used ELUXEO, BL-7000 and VP-7000 LED sources in the experiment. They observed that LED is better than LASER for colour difference value, and LED without image magnification performed better than LASER without magnification. McCallum and Iyer [9] studied the effect of light intensity in endoscopic image quality. They experimented using L9000 LED light source and X800 Xenon Light source to capture ear images. They varied the light intensities in the range of 10%, 30%, 50% and 100% and captured images of the same operative region for 20 patients. They observed that image quality is less concerned with intensity, but reducing the diameter of the light source can reduce the tip temperature. Therefore, a change of light source can help to reduce the temperature.

Natural colour generation in the captured image/video is crucial for medical surgery. The study suggests that LED light is more prominent than LASER light. However, the thermal effect and imaging quality highly depend on the efficacy of the LED source. Therefore, the selection of light plays a critical role in the diagnostic process. This paper presents the study of three different LED sources (a) Type 1 LED: SBM-40 LED [10] (b) Type 2 LED: Cree XLamp®XP-L® Colour LED [11] (c) Type 3 LED: OSRAM OSLON® SSL 80 [12]. Later, an image processing algorithm is presented to increase the contrast of an image. The sigmoid function is used prominently in the image processing area to enhance the scene, image, or object of interest. The least computation cost with better enhancement makes real-time image processing requirements favourable. Therefore, the proposed method enhances global contrast in real-time using a sigmoid function.

2. Materials and Experimental Method

The basic requirements for the MIT are as follows: It requires a small distal tip diameter as far as possible. The end tip should be flexible to cover the large area inside the body. Light sources should consume low power and have high illumination with low heat dissipation. The initial challenge for the LED light source in the endoscopy was the LED light coupling to fiber optic cable. A collimating lens was inserted between the LED source and the fiber to increase the light coupling efficiency [13]. If LED is integrated into the endoscope's tip, the whole luminous flux is available for illumination. However, the LED's petite size does not provide the thermal dissipation of heat, and it is necessary to prevent the heating of the tip. Therefore, heat pipes were incorporated by Brugemann [14] with LED to lower the temperature. This section presents the study on LED sources and camera sensors used in the endoscopy. Initially, the requirement from the LED sources in connection with an endoscope is introduced. Then for the selected LEDs, the detailed experimental method is described.

Generally, narrowband imaging (NBI) is preferred in MIT. Narrowband Imaging increases blood vessel visibility and epithelial tissue structures. Before entering the tissue, NBI light travels through a specific narrow band filter. The filter allows frequencies that match the haemoglobin's absorption spectrum in the blood. Thus, the NBI source selection depends on the wavelength, colour, and Full width half maximum (FWHM) range. According to the NBI system of The Industrial Technology Research Institute of Taiwan, three wavelengths, i.e., Blue, Green, and white, are used in endoscopy. White colour LED allows us to work in bright mode, and endoscope uses typically bright mode [15].

Another mode blends blue and green light to achieve the same effect as the Olympus NBI system. These different imaging modes are shown in figure 1. Figure 1(c) shows four chips, specifically designed for LED sources are assembled on a die. The brightness of each LED can be tuned independently. LEDs are powered using the pulse width modulation (PWM) technique. An analysis of colour rendering from the LED illuminators was presented in [16] to observe the inner surface of the body on the natural colour. The authors used 13 LEDs with different spectral characteristics and analyzed various quality mixing issues of LEDs' colours.

Fig. 1 - (a) NBI LED source PR650; (b) white LED light in the left side and blue/green (mix) LED light in the right side; (c) closed view of blue/green (mix) LED source}

According to the standard defined for NBI, 415 nm and 540 nm centred wavelength was selected for blue and green colour, respectively. The allowed band is 390 nm to 430nm for the blue colour and 520 nm to 560 nm for the blue colour. The presence of chromophores in the Hemoglobin absorbs both blue and green light. This sample light penetration into the tissue for blood vessel identification is shown in figure 2. The blood vessels can seem dark, giving their improved visibility and the enhanced identification of different surface structures.

With this consideration, three manufacturing brands, i.e. Luminous, XLamp, OSRAM OSLON, are identified initially. Cree | Wolfspeed is a semiconductor company working on semiconductor technologies for 30 years. Cree XLamp® LEDs are the best easy-to-use, energy-efficient, and long-lasting LED. For the experiment, the selection of the LED source is essential. Therefore, a comparison of parameters for the various LEDs for each brand is established. The following table 1 presents the LED sources matching with the NBI standard. The drive current and power required for the LED are essential parameters in selecting the light source. Therefore, the XP-L LED source from the Cree is selected in the proposed experiment.

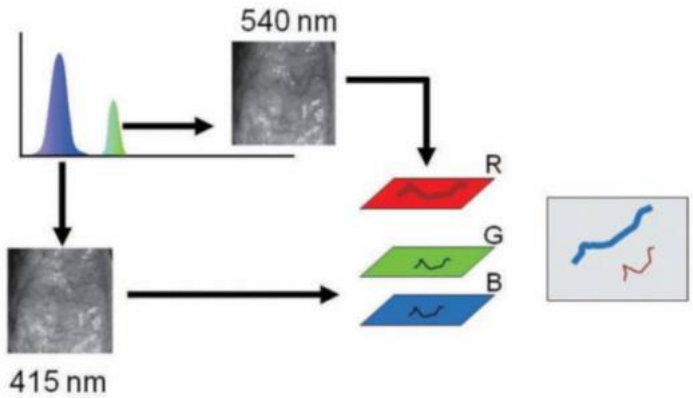

Fig. 2 - Penetration of light into tissues and blood vessels visibility (Image courtesy of Olympus R & D, Japan, adopted from [17])

Table 1 - LED sources from Cree XLamp and their comparison

Type / Model No	Size (mm)	Max Illuminance (lm)	Viewing angle	Forward Voltage	Max Power (W)	Max Drive Current (A)
XHP50.2	5 X 5	2654	120	5.6@1400 mA	18	3
XP-L2	3.45 X 3.45	1175	125	2.82 @1050 mA	10	3
XP-L	3.45 X 3.45	1150	125	2.95 @1.05 A	10	3
XHP35	3.45 X 3.45	1833	125	11.3 @350 mA	13	1.05
XHP50	5 X 5	2546	120	5.75 @1400 mA	19	3

Similarly, the ILS PowerStar brand uses the OSLON LEDs with different viewing angles, i.e., 80 degrees, 150 degrees. Their performance is consistent even at maximum drive current and offers low thermal resistance. And Luminous brand's LEDs are high thermal conductivity and can be operated in the range of 0.1 A to 1.0 A driving current. The comparison for both brands is listed in table 2. SSL-80 and SBM-40 are selected from OSLON and Luminous in the proposed experiment.

Table 2 - OSLON and Luminous LED Sources

Model No	Colour	Wavelength (nm)		Current(A)	FWHM (nm)	
		Blue	Green		Blue	Green
Luminous SBM-40-LC	RGBW	452-457	524-529	1	21	32
Luminous SBT-70	GB	435-455	520-540	10.5	19	32
Luminous SBM-40	RGBW	449-457	521-533	2	21	32
OSLON 80 SSL Power-Star	RGBW	470	528	1	-	-
OSLON 150	RGBW	470	528	1	-	-

2.1 Measurement Procedure

A borescope is used to examine the LED's illuminance. There are two types of borescope: flexible and rigid. A rigid borescope is suitable for the applications requiring straight-line access in the target inspection. However, they don't fit well to inspect objects with unusual internal cavities. A flexible borescope has a movable and adjustable shaft. This shaft can quickly enter hard-to-reach places inside the body. Compared to rigid borescopes, flexible borescopes send images by compact, lightweight fiber bundles [18]. Therefore, the proposed experiment uses a borescope with a flexible tip to quantify the illuminance. The block diagram for the LED test setup is shown in figure 3.

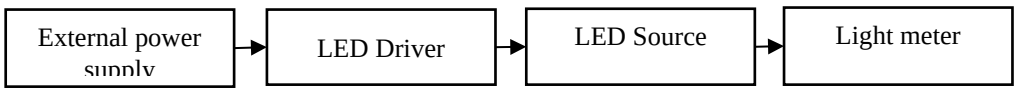

Fig. 3 - Block diagram for LED illuminance measurement

A steady voltage and current are generated using the external power supply. LEDs are intended to keep running at low voltage. An LED driver rectifies a higher voltage to the voltage sustained by the LED. LED driver circuit additionally shields LEDs from a voltage or current vacillations. The variation in the supply voltage causes the change in the LED's current, and the LED emits the light according to the supplied current. As a precaution, LEDs are evaluated to work within a specific current range according to the specifications provided by the brands (estimated in amps). The light meter is utilized to estimate the light force of the borescope at various separations.

(a) The LED's illuminance measurement:

For testing LEDs, an optical bench is prepared with two stands. One stand is fixed in the position, and the second stand is movable to change the distance and measure the light's illuminance in the variance of the length. To prevent the insertion of the surrounding external light, LED and lux meters are covered with paper cones. Further, the inefficient semiconductor process also produces heat within the device while producing light. To dissipate heat, mounting the heat sink is essential. Kells et al. [19] used a 12V DC fan and a heat sink to dissipate heat and increase the airflow. In the proposed prototype, heat sinks are mounted with LED. Figure 4 shows the developed prototype model.

The LED's illuminance measurement procedure is as follows:

- Remove the protective cap from the sensor to expose the white-domed light sensor to the light.
- Press the LUX button to select lux units or the Fc button to select foot candle units.
- Press the RANGE button to select the range that provides the maximum resolution.
- Put the 3D fixture on a white-domed light sensor and insert the borescope's distal end into the 3D fixture hole.
- Set borescope at maximum distance and measure the reading. Then measure changes in the illuminance with changes in the current.
- Similarly, study the changes in the LED's illuminance by varying the current range (i.e., in the proposed setup, the used current range is 50 mA to 800 mA).

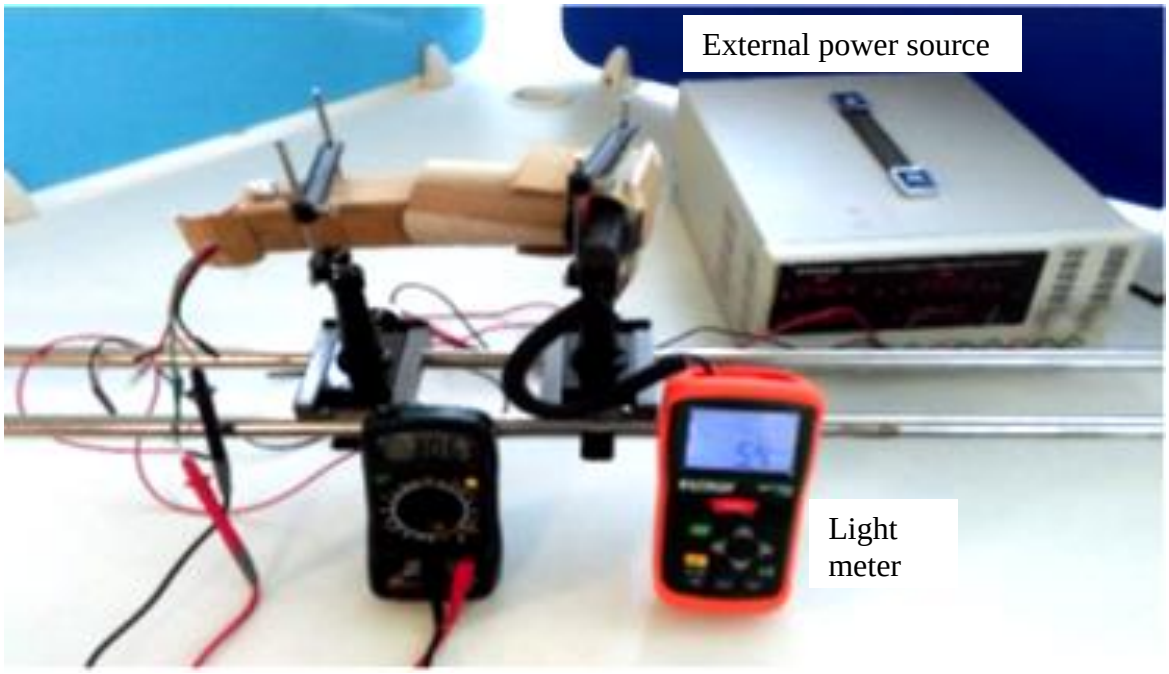

Fig. 4 - Proposed test setup for LED illuminance

(b) Wavelength measurement of LED source:

Further, the wavelength is analyzed for each LED. The reflection properties of the tissues or organs play an essential role to discriminate the suspicious tissues from the normal tissues. Therefore, the reflection property is used for light source selection. Shen et al. [20] presented the benefits of spectral reflectance. The objective was to find the wavelength producing the highest contrast between background tissues and blood vessels. The blue and green colours are the vital spectrum as per NBI guidelines. Aligned wavelengths with the human eye's sensitivity can improve the Luminous Efficacy of Radiation [21]. Therefore, the experiment measures the LED's wavelength and FWHM (in nm) using the wavelength meter. The wavelength meter has two ports: one input port senses the light through the fiber cable from the integrated sphere. The second output port connects the wavelength meter to the computer using a USB cable to record it. The designed test setup used in the experiment is shown in figure 5.

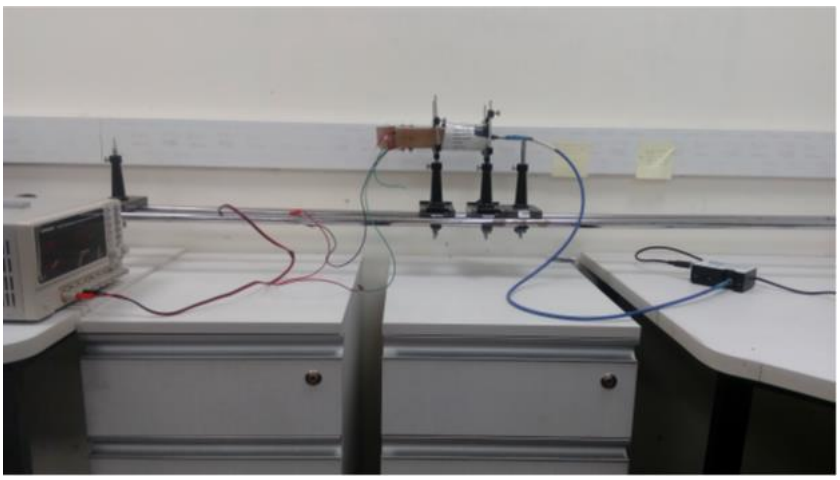

Fig. 5 - Test setup to analyze the wavelength and FWHM of LED

The wavelength measurement procedure is as follows:

- Setup the optical bench, as shown in figure 5. Fix the light meter at one end and fix the portable LED at the second end of the bench.
- Connect the fiber cable from the integrated sphere to the wavelength meter and from the wavelength meter to the computer.
- Heat sinks are mounted with LED to prevent the dissipation of the heat from the LED.

- Fixed the input voltage and measured the wavelength by varying the current (i.e., from 50 mA to 800 mA)

In endoscopy, imaging algorithm also plays an important role. Imaging applications include three chips: a picture sensor, a simple front-end (AFE), and an advanced ASIC. The picture sensor captures images, and the AFE module is an interface for the digital and analogue sensor. AFE enables the picture to break down and its improvement. Overall, digital image formation in the endoscopy is shown in figure 6.

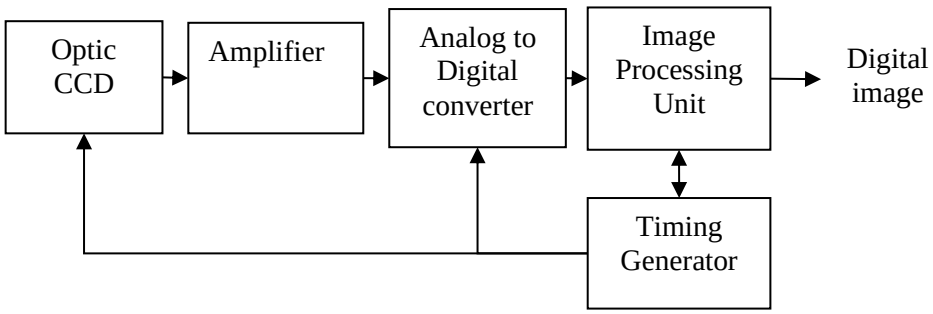

Fig. 6 - Camera's image processing (adapted from [22])

In figure 6, the image sensor captures images at a specific rate and acts as input to AFE. AFE conditions the sensor's electrical signal and converts an analogue image into a digital image. AFE gives Digital output (voltages) with dark current cancellation, reset level variations, defective pixel correction, and DC offset variations. The image processing unit processes the digital image using various filtering approaches to correct the colour information according to the human visual system.

The most widely recognized sensors are the charge-coupled device (CCD) and complementary metal-oxide-semiconductor (CMOS). Every pixel has its particular charge-to-voltage transformation in the CMOS sensor, and the sensor also incorporates amplifiers, clamour rectification, and digitization circuits. These features permit the rapid transfer of high aggregate data.

CCDs utilize a worldwide shade, which uncovered the whole picture simultaneously. As a result, CCD has better light sensitivity and can generate low-noise and high-quality images at the cost of considerable power and high cost [23]. On the other hand, compared with CCD, CMOS sensor cost less and consumes less power with lower light sensitivity and less resolution. Table 3 shows an overall comparison of the CCD and CMOS.

Table 3 - Parameter comparison between CCD and CMOS

Parameter	CCD	CMOS
Pixel signal	Electron packet	Voltage
Chip signal	Analog	Digital
Noise level	Low	Moderate - High
Uniformity	High	Low
Speed	Moderate- High	High
Power consumption	Moderate- High	High
Circuit Complexity	Low	Moderate
Cost	Moderate	Low-moderate

CMOS sensor is better than the CCD sensor for endoscope application due to less power requirement (less heating) and high-speed data transmission rate. However, due to low resolution, it requires post-processing of the captured image. Two types of systems are used to generate NBI images. Firstly, the RGB illumination [24], where a narrow spectrum of three primary colours discussed in section 2 is used to obtain true colour tissue images. Secondly, the AFI system where a rotating wheel of the colour filter is placed in front of the light source generating blue and green colour sequentially [25]. However, both these systems increase the complexity of hardware and power consumption. Therefore, various researchers also proposed global and self-adaptive image processing algorithms to enhance the image's contrast in real-time. Histogram equalization and its run-time modification [26-27], high boost filtering [28], and fuzzy method based histogram equalization [29] are a few examples of these real-time algorithms. These adaptive methods process image pixels in the local region or block of the image and use neighbouring pixels to remove the artefact in that region. However, it may lead to boosting noise too in the smooth areas.

Moreover, the high boost filtering boosts the high-frequency components, i.e., edge inclusive of low-frequency components, i.e., smooth regions causing distortion. This paper proposed real-time image enhancement without

incorporating additional hardware and memory complexity. The block diagram of the image enhancement algorithm, which works in real-time, is presented in figure 7.

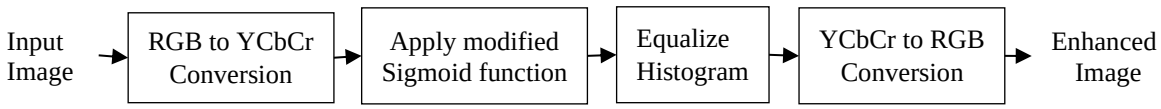

Fig. 7 - Block diagram of the image enhancement algorithm

The first step is converting the RGB colour map to the HSV colour map. Next, the luminance component (Y) of YCbCr is used to enhance the image pixel, and the chrominance component maintains the colour map of the RGB image. Then all image components' range is normalized to [0, 1] using equation 1.

$$Y_{norm} = \frac{Y - Y_{min}}{Y_{max} - Y_{min}} \quad (1)$$

Where Y_{min} and Y_{max} are minimum and maximum intensity values within the image plane. After this process, a modified sigmoid function proposed in [30] is used to manipulate the pixel's intensity and enhance an image. The standard sigmoid function for an image Y_{norm} is given by

$$Sig(x,y) = \frac{1}{1+\exp(-Y_{norm}(x,y))} \quad (2)$$

Enhancing the specific region containing mucosa structure requires the controlling of exponent function. Therefore, gain (g) and threshold factor (T) are introduced in the modified sigmoid function as follows:

$$Sig(x,y) = \frac{1}{1+\exp(g(-Y_{norm}(x,y)-T))} \quad (3)$$

Two parameters, g and T, control the brightness and contrast of an image. Several combinations of g and T are used to obtain the optimum value, and corresponding PSNR values are calculated. Finally, the optimum value-generating maximum PSNR is selected to enhance the image. The following section presents the testing of LEDs and image processing algorithm, and corresponding results are discussed.

3. Results analysis

This section presents the illuminance and wavelength analysis of LED.

3.1 Illuminance measurement and analysis

In the test setup, distance is varied manually from the light source, and the corresponding illuminance is measured using the borescope. The illuminance is measured at every 2 mm step, shown in figure 8. Figure 8 shows that the illuminance is inversely proportional to the distance. And the maximum illuminance of 5.85 Klux is obtained from the measurement.

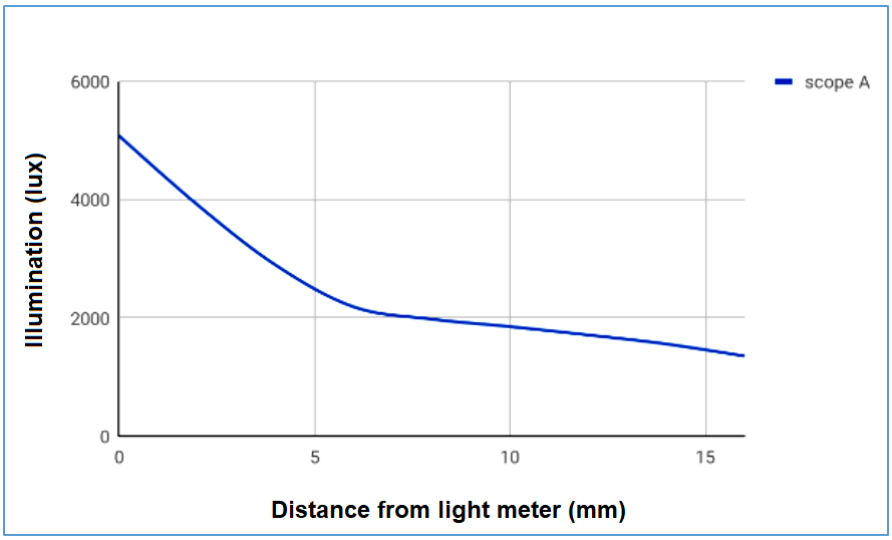

Fig. 8 - Light source illuminance vs distance for type 1 LED

A second analysis of LED is to observe the effect of driving current on the LED's illuminance. The distance between the light source and the borescope has been fixed, and the effect is analyzed by measuring the LED's illuminance at different driving currents. Figure 9 shows the white colour illuminance variation of type 1 LED with variation in the

driving current. The increment in the driving current causes an increment in the illuminance. With this measurement, the comparative analysis for the white, green, and blue colour's illuminance comparison between selected brands are presented in figure 10.

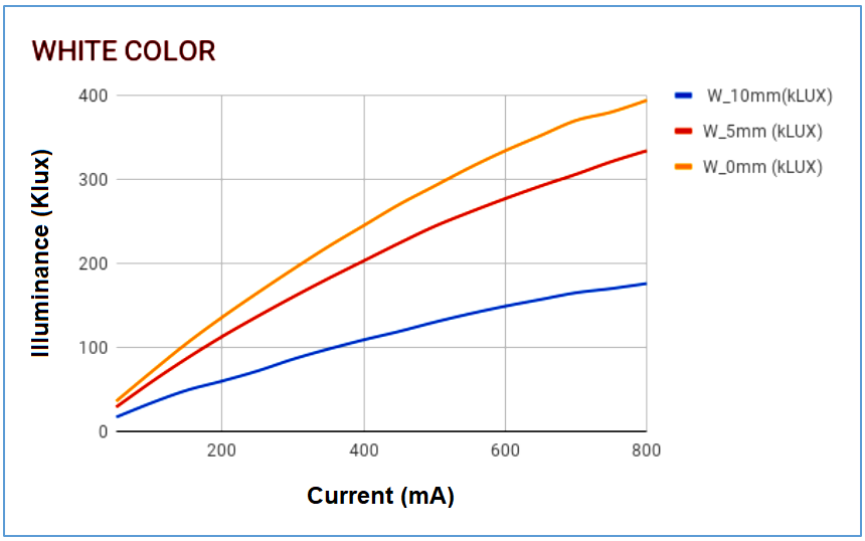

Fig. 9 - White colour illuminance versus the driving current for type 1 LED

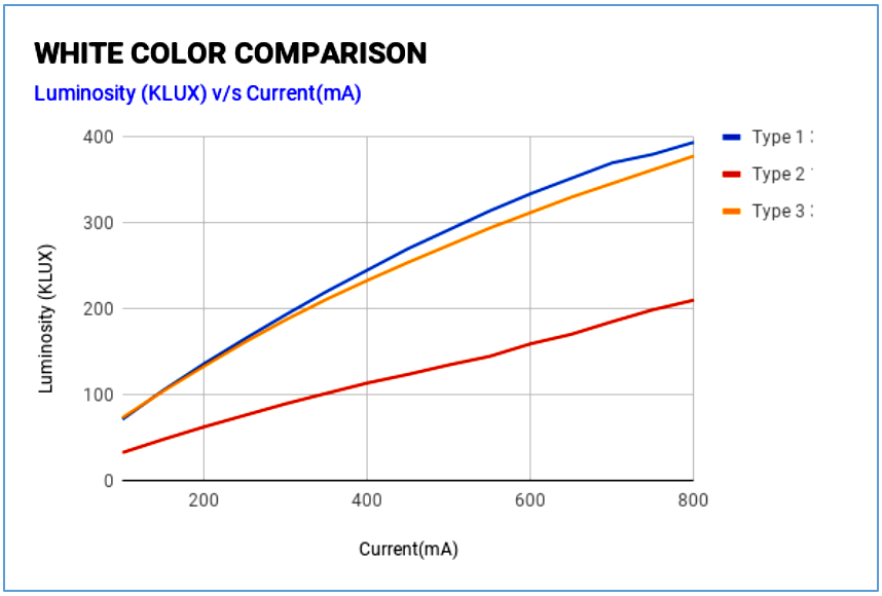

Fig. 10 - White colour illuminance comparison amongst three types of LED

3.2 Spectrum analysis and wavelength measurement

The test setup described in figure 5 is used to measure the wavelength of each LED. This spectral composition differentiates the region of interest (i.e., the appearance of suspicious tissues) from the surrounding area (i.e., normal tissues can be considered background). Tissues usually reflect the wavelength of 450 nm to 550 nm generating high contrast grey colour images [31]. By varying the integration time, green and blue colour illuminance is measured for each LED type. The recorded values are presented in table 4. Spectrum comparison of all three LEDs is shown in figure 11. Figure 11 shows that all LEDs fulfil the requirement of the NBI standard for each colour spectrum. Utilizing a digital filter in AFE (i.e., figure 7) can improve the obtained spectrum. Looking at the requirement of endoscopy, type 3 LED is better than the other two types.

Table 4 - Blue and Green colour wavelength analysis for three LEDs

Parameter	Luminosity (Klux)			FWHM (nm)			Peak wave length(nm)		
LED Type	Type 1	Type 2	Type 3	Type 1	Type 2	Type 3	Type 1	Type 2	Type 3
Blue Colour	1.6	0.2	1.2	17.8	22.9	18	461.38	461.76	446.83
Green Colour	1.3	0.6	1.5	31.62	29.64	33.68	517.7	522.77	622.05

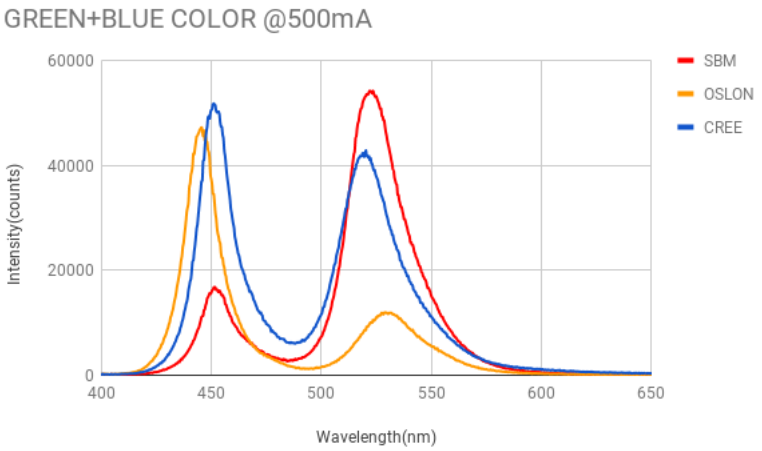

Fig. 11 - Spectrum comparison for Green and Blue colour wavelength

4. Contrast Enhancement and True Colour Image Generation

The image processing algorithm's observation is shown in figure 12. A reference image shown in figure 12 represents the inner surface of mucosa where actually disease is occurring, and it is captured during the endoscopy procedure.

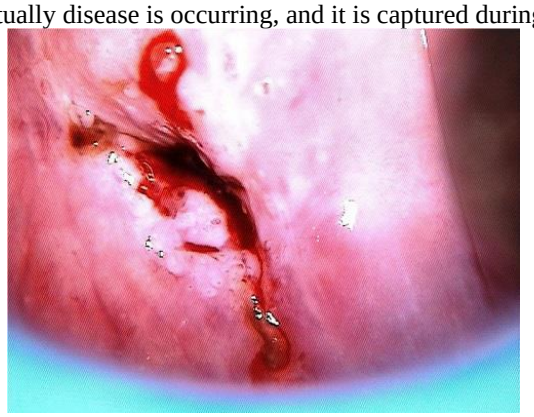

Fig. 12 - Reference images: the inner surface of the mucosa

The image is converted to a YCbCr in the first step to reduce the computation cost. The luminance component Y is very similar to the grey colour version of the colour image. CbCr represents colour information with a small volume of data compared to RGB colour space. Then to accomplish consistency in the image plane, all components are normalized using equation 1. Later a modified sigmoid function is applied to the luminance component to enhance an image. The following figure 13 compares the original sigmoid function (i.e., using equation 2) and modified sigmoid function using (i.e., using equation 3).

In medical images, mucosa and tissues enhancement is required since the experts require an investigation. Therefore, the endoscopy image in the YCbCr domain is applied to this modified sigmoid function adjusting its contrast and brightness for better characterization. After using the modified sigmoid function, the original colour is reproduced by converting the YCbCr's colour map to RGB.

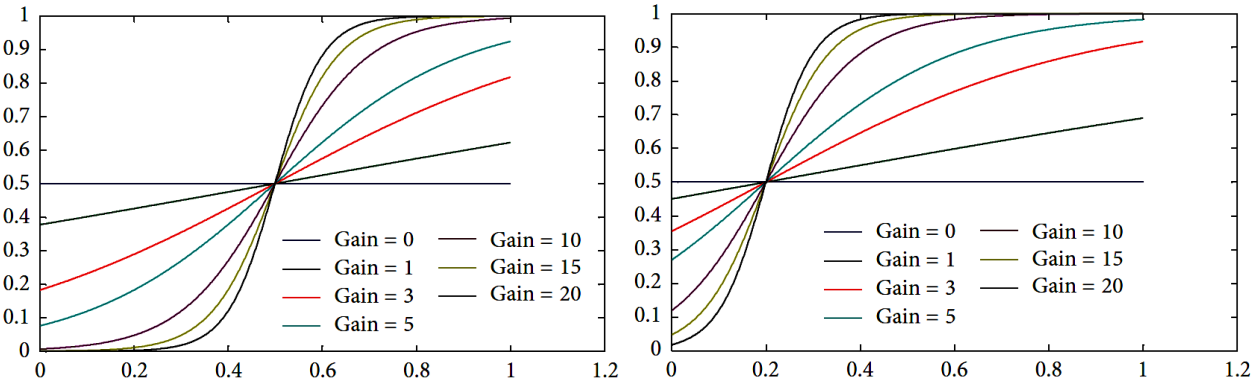

Fig. 13 - (a) Original sigmoid function using equation 2 (b) modified sigmoid function using equation 2

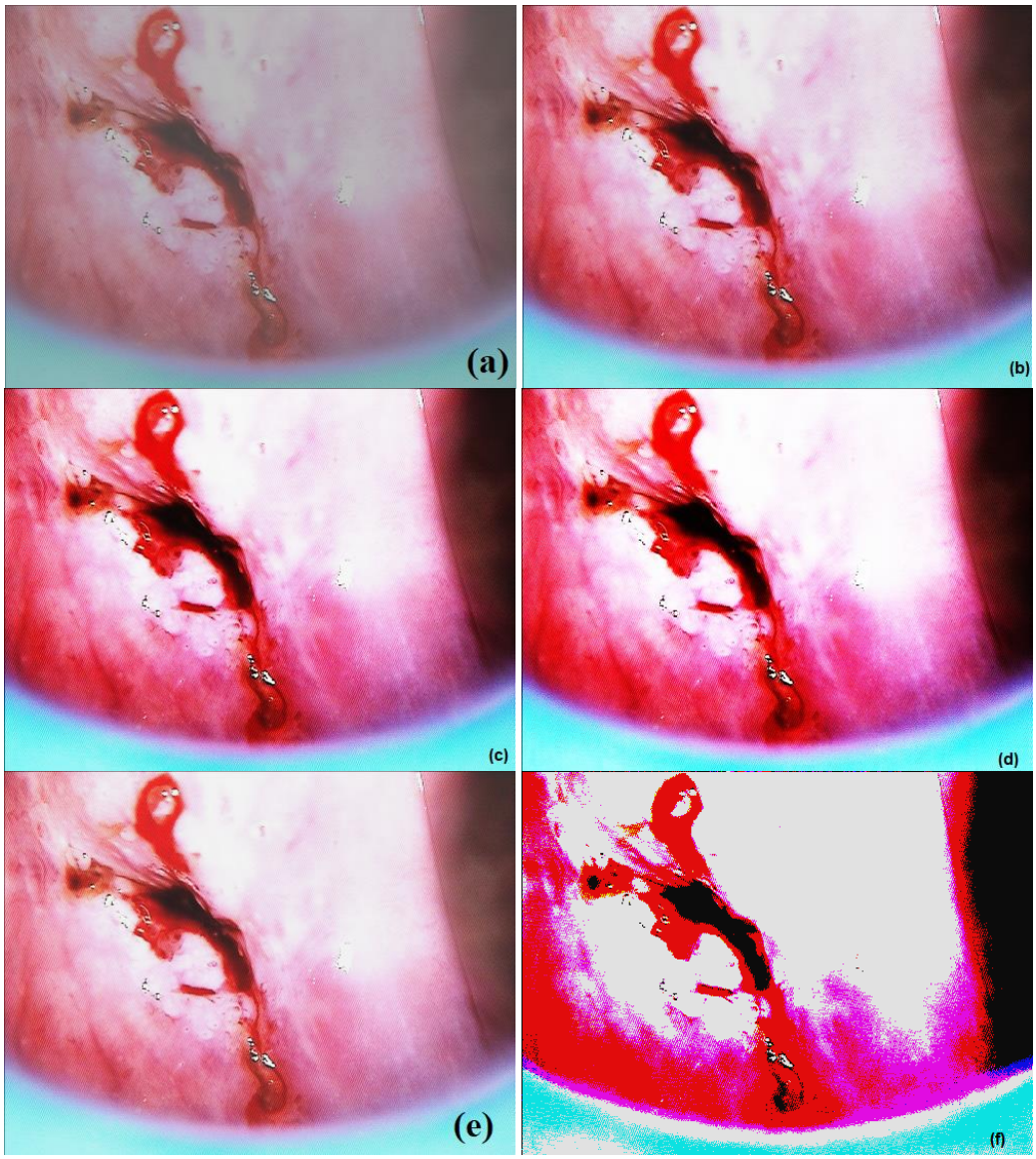

Fig. 14 - Results obtained for various combination of g and T from figure 13 (a) T= 0.5, g = 2 (b)T= 0.5, g = 5 (c) T= 0.5, g = 7 (d) T= 0.5, g = 10 (e)T= 0.4, g = 5 (f)T= 0.6, g = 5

Figure 14 represent the enhanced images after using the various combination of g and T. The right combination of T and g is vital for better image enhancement, i.e., enhancing mucosa structure and keeping true colour to rest tissues. Therefore, as suggested, the sigmoid function is analyzed using peak signal to noise ratio (PSNR). The camera sensor's noise and illuminance obtained from the LED source produce a different dynamic range, changing the image quality.

PSNR is the ratio of the maximum power of an image to the power of noise affecting the image quality. Thus, the image is quantified as better enhanced if higher PSNR is obtained. The PSNR value analysis is carried out by changing the values of g, and T. Figure 15 represents the obtained PSNR for a few combinations of g, and T. Figure 15 suggests that for g = 5 and T = 0.5, maximum PSNR is obtained for the mucosa image. The corresponding image is shown in figure 14e, which is more similar to true images with mucosa structure enhancement. Thus, a better-enhanced image can be obtained compared to other combinations using this combination.

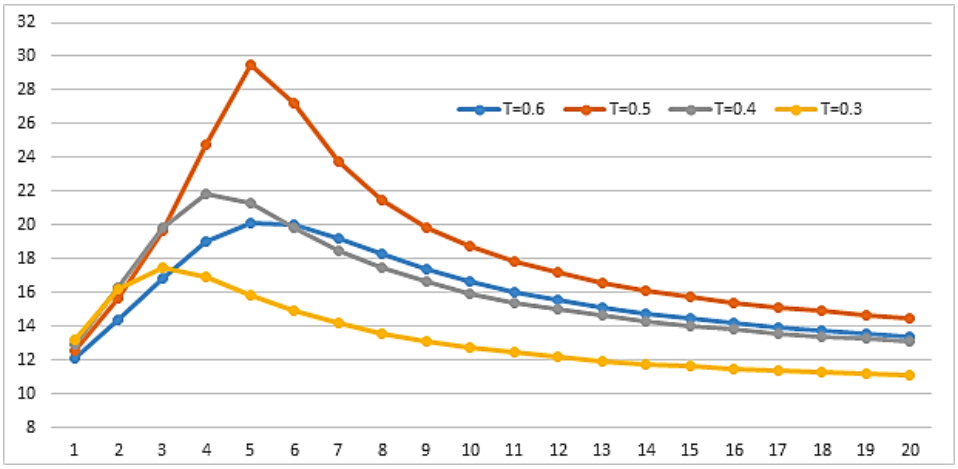

Fig. 15 - Calculated PSNR of enhanced image for various combinations of g and T in sigmoid function (X-axis: g and Y-axis: PSNR in dB)

Further analysis of proposed image enhancement using various combinations of g and T is performed in different endoscopy images obtained from Gastolab [36]. The samples images and enhanced images are shown in figure 16.

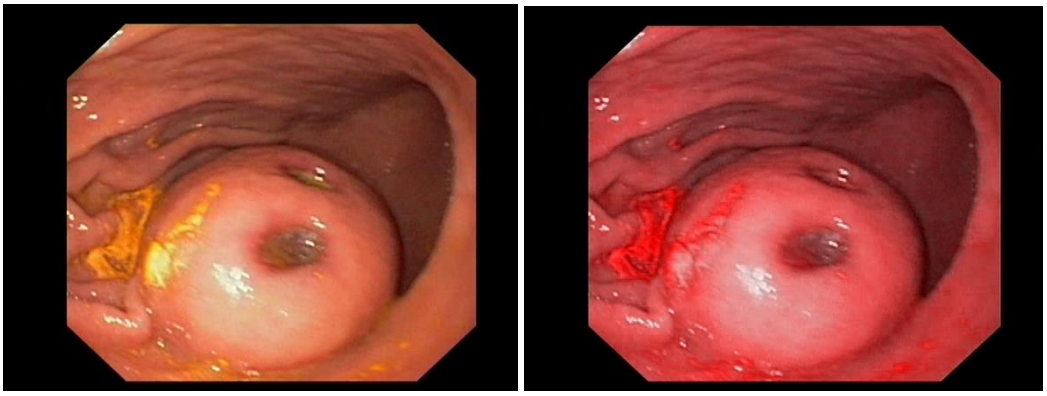

(a) Ulcertic gastric image and its enhancement (PSNR = 33.39 dB)

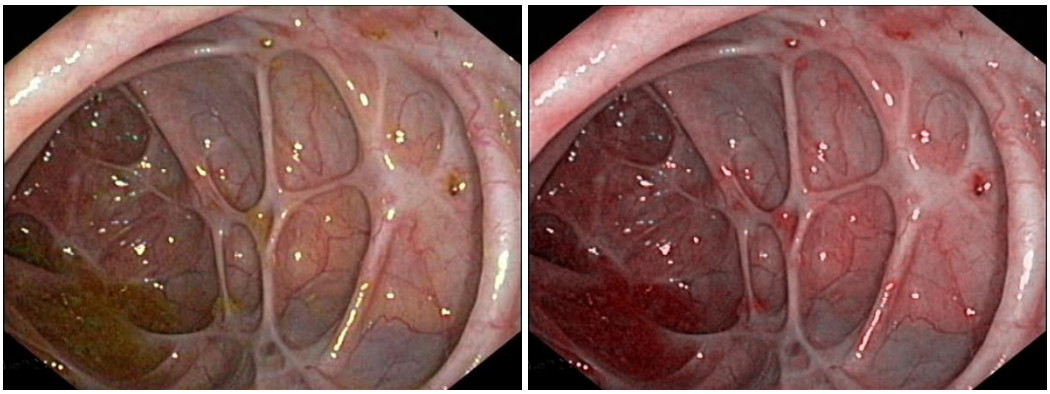

(b) Ulcertic Mucosa image and its enhancement (PSNR = 34.12 dB)

Fig. 16 Sample endoscopy images and their enhancement using the proper combination of g and T

Figure 16 shows that the adaptive sigmoid function makes images visually better and does not generate new colours in the image. The ulcerative region in both sample images is enhanced with a better PSNR value. To establish comparative

analysis, a mean value of PSNR of all images is calculated and compared with previous literature presenting real-time endoscopic image enhancement. The following table 5 shows this comparison. In [32], a deep learning framework was presented to classify six types of artefacts and to enhance endoscopic images. Their model successfully obtained 25.72 dB mean PSNR, and the average computation time was 88 ms. Zhang et al. [33] presented a weighted guided filtering framework for image enhancement in terms of brightness and contrast. For enhancement, they extracted the base layer from R, G, and B components using weighted filtering and obtained a details layer by substracting this base layer from three colour components. Later they enhanced these details layers and merged them back to colour components. A wireless camera is used for capsule endoscopy in [34] for 30 images. They presented a stochastic sampling and edge-based smoothing framework to enhance the image details and texture of tissues in this paper. However, this method is not fast enough for real-time execution. Gomez Pablo et al. [35] presented a low-light image enhancement using HSV components. They used Perlin noise to darken images, and U-Net architecture was demonstrated to enhance these dark images. However, they succeed to achieve PSNR 23.79 dB. The comparison states that the proposed framework offers the least computation and performs better PSNR.

Table 5 A comparative analysis of real-time endoscopic image enhancement using mean PSNR

Method	Average PSNR
Deep Learning [32]	25.72
Wighted Guided filtering [33]	32.60
Capsule endoscopy [34]	32.45
U-Net [35]	23.79
Proposed method	**34.25**

5. Conclusion

An endoscope is the most effective and safe tool in diagnosing the inner body region. The effectiveness of the endoscopy depends on the acquisition of images/videos inside the body region. LEDs offer many advantages over incandescent and fluorescent lights, including compact, highly efficient and digitally controlled. However, selecting an LED light source and camera plays an essential role in endoscopy. This paper presented a study on the parameters of LED light sources playing a vital role in capturing inner body region images. Initially, a comparative study on various LED sources from three popular brands are presented, and three LEDs based on the driving current and power requirement is selected for experimentation. The appropriate LED spectrum provides a colour gamut of displays. The driving current and ambient temperature can cause a change in the spectrum. A low-cost prototype model testing these LED sources is developed and presented in this paper to select an appropriate LED. Rigorous analysis of LEDs is carried out using their spectrum analysis. A comparative study is presented measuring source illuminance over the distance, white colour illuminance over the driving current, and a blue-green colour wavelength analysis. The experiment study showed that type 3 LED was better to satisfy the NBI standards and produce higher illuminance with less heating. Later, a comparative study between the camera sensor, i.e., CCD and CMOS, is established, and it is found that CCD produces high contrast images compared to CMOS. However, CMOS has the advantages of being low-cost and high-speed. A simple image processing algorithm is also proposed to enhance the image's contrast in real-time. A sigmoid function is modified to enhance the colour. The algorithm is applied to enhance the mucosa's inner structure. An appropriate selection of the controlling parameters in adaptive sigmoid function provided a mean PSNR of 34.25 dB. The proposed framework does not add colour to the true image and generates an enhanced image without any computation cost.

Acknowledgement

The authors declare that they have no conflict of interest.

References

[1] P. Belloni, A. Gartner (2017) Challenges when Designing LED-Based Illumination Systems in Medical Applications and Diagnostics, 1st edn.

[2] Wehby, H., Wadaane, M., Wehbi, H., Khayreldeen, M., ElSayed, A., HajjHassan, M., ... & Rashwani, K. (2021). 100-watt MATLAB/Simulink Model LED Based Light Source for Medical Endoscopy. 1st International Conference on Emerging Smart Technologies and Applications (eSmarTA), 1-6. IEEE.

[3] Afyouni, A., O'Leary, M., Okhunov, Z., Peta, A., Brevik, A., Ayad, M., ... & Clayman, R. (2021). Mp67-16 Long-Term Impact Of The Endockscope System: A Global Assessment. The Journal of Urology, 206, e515-e516.

[4] Takayama, S., Dohi, O., Naito, Y., Azuma, Y., Ishida, T., Kitae, H., ... & Itoh, Y. (2021). Diagnostic ability of magnifying blue light imaging with a light emitting diode light source for early gastric cancer: a prospective comparative study. Digestion, 102(4), 580-589.

[5] Mueller, J. L., Rozman, N., Sunassee, E. D., Gupta, A., Schuval, C., Biswas, A., ... & Fitzgerald, T. N. (2021). An Accessible Laparoscope for Surgery in Low-and Middle-Income Countries. Annals of biomedical engineering, 49(7), 1657-1669.
[6] R. F. R. Suélia de Siqueira, I. João Yoshiyuki and G. R. Oscar Fernando (2019). Embedded System for Lighting Control of LED Light Source Applied to Therapy of Radiofrequency Ablation in Hepatocellular Carcinoma," in IEEE Latin America Transactions, 17(10), 1671-1677
[7] Yu, F., Song, E., Liu, H., Li, Y., Zhu, J., & Hung, C. C. (2018). An augmented reality endoscope system for ureter position detection. Journal of Medical Systems, 42(8), 1-12.
[8] Yoshida, N., Dohi, O., Inoue, K. et al. (2020). The efficacy of tumor characterization and tumor detectability of linked color imaging and blue laser imaging with an LED endoscope compared to a LASER endoscope. International Journal of Colorectal Disease, 35, 815–825.
[9] McCallum, R., McColl, J., & Iyer, A. (2018). The effect of light intensity on image quality in endoscopic ear surgery. Clinical Otolaryngology, 43(5), 1266-1272.
[10] Luminus Devices Inc., Luminus SBM40 LED (https://www.mouser.com/datasheet/2/245/Luminus_SBM40_Datasheet-540764.pdf)
[11] Cree Inc., XLamp® XM-L® Colour LED (https://www.cree.com/led-components/media/documents/XLampXML_Colour.pdf)
[12] Intelligent LED Solutions, OSRAM OSLON® SSL 80 (https://i-led.co.uk/PDFs/OSLON/OslonRGB80+SSLPowerStarV1.0.pdf)
[13] Rooman, C., Kuijk, M., Vounckx, R. A., & Heremans, P. L. (2005). Reflective-refractive microlens for efficient light-emitting-diode-to-fiber coupling. Optical Engineering, 44(9), 095005.
[14] D. Bruggemann (2014) Development and construction of a video endoscope with integrated led light sources. Ph.D. thesis, Technical University.
[15] Chang, H. J., Wang, W. H., Chang, Y. L., Jeng, T. R., Wu, C. T., Angot, L.,Wang, P. C. (2015). Light-emitting diode-assisted narrowband imaging video endoscopy system in head and neck cancer. Clinical endoscopy, 48(2), 142-146.
[16] Blaszczak, U. J., Gryko, L., Palkowska, A., Kulesza, E., & Zajac, A. (2016). Colour mixing in LED illuminating system for endoscopic purposes. IEEE Lighting Conference of the Visegrad Countries (Lumen V4). 1-6.
[17] Srivastava, R. (2019). History and Physics of Narrow Band Imaging. In Atlas on Narrow Band Imaging in Upper Aerodigestive Tract Lesions, 7-10, Springer, Singapore.
[18] Scholly Excellence Inside, Endoscope versus Borescope (https://www.schoelly.de/en/visual-inspection/industry-report/endoscope-versus-borescope/)
[19] Kells, K. R., Kong, K. Y., White, W. B., Kaddi, C., & Wang, M. D. (2013). LED light source for fluorescence endoscopy using quantum dots. In 2013 IEEE Point-of-Care Healthcare Technologies, 9-12, IEEE.
[20] Shen, J., Wang, H., Wu, Y., Li, A., Chen, C., & Zheng, Z. (2015). Surgical lighting with contrast enhancement based on spectral reflectance comparison and entropy analysis. Journal of biomedical optics, 20(10), 105012.
[21] Liu, A., Khanna, A., Dutta, P. S., & Shur, M. (2015). Red-blue-green solid state light sources using a narrow line-width green phosphor. Optics express, 23(7), A309-A315.
[22] Buckley, K. (2000). Selecting an analog front-end for imaging applications. Analog Dialogue, 34(6), 40-44.
[23] HowStu_Works, Difference between CCD and CMOS (http://electronics.howstuffworks.com/cameras-photography/digital/question362.html)
[24] Kuznetsov, K., Lambert, R., & Rey, J. F. (2006). Narrowband imaging: potential and limitations, endoscopy, 38(01), 76-81.
[25] Schmitz-Valckenberg, S., Holz, F. G., Bird, A. C., & Spaide, R. F. (2008). Fundus autofluorescence imaging: review and perspectives. Retina, 28(3), 385-409.
[26] Pizer, S. M., Amburn, E. P., Austin, J. D., Cromartie, R., Geselowitz, A., Greer, T., ... & Zuiderveld, K. (1987). Adaptive histogram equalization and its variations. Computer vision, graphics, and image processing, 39(3), 355-368.
[27] Jenifer, S., Parasuraman, S., & Kadirvelu, A. (2016). Contrast enhancement and brightness preserving of digital mammograms using fuzzy clipped contrast-limited adaptive histogram equalization algorithm. Applied Soft Computing, 42, 167-177.
[28] Srivastava, R., Gupta, J. R. P., Parthasarthy, H., & Srivastava, S. (2009). PDE based unsharp masking, crispening and high boost filtering of digital images. In International Conference on Contemporary Computing, 8-13, Springer, Berlin, Heidelberg.
[29] Sheet, D., Garud, H., Suveer, A., Mahadevappa, M., & Chatterjee, J. (2010). Brightness preserving dynamic fuzzy histogram equalization. IEEE Transactions on Consumer Electronics, 56(4), 2475-2480.
[30] Imtiaz, M. S., & Wahid, K. A. (2015). Color enhancement in endoscopic images using adaptive sigmoid function and space variant color reproduction. Computational and mathematical methods in medicine, Article ID 607407, 1-19.

[31] Clancy, N. T., Li, R., Rogers, K., Driscoll, P., Excel, P., Yandle, R., & Elson, D. S. (2012). Development and evaluation of a light-emitting diode endoscopic light source, Advanced Biomedical and Clinical Diagnostic Systems X, International Society for Optics and Photonics, 8214, 1-13.
[32] Ali, S., Zhou, F., Bailey, A., Braden, B., East, J. E., Lu, X., & Rittscher, J. (2021). A deep learning framework for quality assessment and restoration in video endoscopy. Medical Image Analysis, 68, 101900, 1-25.
[33] Zhang, G., Lin, J., Cao, E., Pang, Y., & Sun, W. (2022). Research on Tissue Structure Enhancement Method of Medical Endoscope Images, Research Square, 1-24.
[34] Mohammed, A., Farup, I., Pedersen, M., Hovde, Ø., & Yildirim Yayilgan, S. (2018). Stochastic capsule endoscopy image enhancement. Journal of Imaging, 4(6), 75, 1-20.
[35] Gómez, P., Semmler, M., Schützenberger, A., Bohr, C., & Döllinger, M. (2019). Low-Light Enhancement of High-Speed Endoscopic Video using a Convolutional Neural Network, 1-5.
[36] Gastrolab—The Gastrointestinal Site, http://www.gastrolab.net/gall139.htm